

Spacecraft Protective Structures Design Optimization

Robert A. Mog*

Science Applications International Corporation, Huntsville, Alabama 35806

The optimization of spacecraft protective structures designed to defeat hypervelocity impacts of meteoroids and space debris is presented. A space debris environment model is incorporated into an overall optimization methodology employing engineering models developed to predict protective structures design requirements for hypervelocity impact loads. Several nonlinear optimization techniques are used to generate design parametrics based on environment, mission, and configuration variables for the Space Station core module configuration. Results indicate that careful consideration of the spacecraft structural configuration and materials can partially offset the design consequences of dramatic increases in the orbital space debris environment. Furthermore, the use of nonlinear optimization techniques coupled with hypervelocity impact engineering models can provide significant design tradeoff insight through the use of parametric analyses.

Nomenclature

A	= spacecraft space debris area
B	= spacecraft orientation factor
C	= bumper material speed of sound
D	= projectile diameter
e	= bumper elongation
f	= non-normalized impact velocity distribution
f_n	= normalized impact velocity distribution
F	= space debris flux
h	= spacecraft altitude
i	= spacecraft inclination
K	= penalty function acceleration factor
L_2	= wall material constant
m	= projectile mass
N	= cumulative space debris flux
N_1	= number of walls penetrated (normal impact)
N_F	= number of walls penetrated by flight-path debris (oblique impact)
N_N	= number of walls penetrated by normal-path debris (oblique impact)
P_0	= spacecraft probability of no penetration
p	= space debris growth rate
R_p	= projectile radius
S	= bumper/wall separation
S_{y1}	= bumper yield strength
S_{y2}	= wall yield strength
s	= solar flux
T	= mission duration
t_1	= bumper thickness
t_2	= wall thickness
V	= projectile impact velocity
V_{\max}	= maximum space debris impact velocity
W	= structure mass per unit area or weight
δ	= discrete penalty function coefficient
δ_i	= dual variable for geometric programming
ϵ	= convergence parameter for random search
θ	= impact angle from surface normal
ν	= dual objective function for geometric programming

ρ_1	= bumper density
ρ_2	= wall density
ρ_p	= projectile mass density
ϕ	= penalty objective function
Ψ	= spacecraft inclination factor

I. Introduction

A. Problem Statement

S SPACECRAFT designers have been concerned since the 1960s about the effects of meteoroid impacts on mission safety. The meteoroid environment has been well documented by Cour-Palais¹ and Susko.² Recent concerns have extended to the space debris environment, which typically displays more massive particles than the meteoroid environment for the same risk level. Additionally, the higher exposure area-time product of future space missions (e.g., Space Station) poses a more critical design problem than current short-term missions. Finally, the inherent uncertainties in projectile mass, velocity, density, shape, and impact angle make the traditional deterministic design approach obsolete.

The engineering solution to this design problem has generally been to erect a bumper or shield spaced outboard from the spacecraft wall to disrupt/deflect the incoming projectiles. This passive measure has resulted in significant structural weight savings relative to a single wall concept with the same protective capability. This advantage of bumper/wall systems to single wall concepts has been shown by a number of investigators, including Madden,³ Nysmith,⁴ Swift,⁵ and Wilkinson.⁶ Additionally, Richardson⁷ has developed empirical equations for a double bumper/wall configuration. The problem, then, is how to efficiently design these protective structures so that the bumper disrupts the projectile without posing a lethality problem to the wall, which serves to protect the crew and equipment.

Spacecraft designers have a number of tools at their disposal, which aid in the design process. These include hypervelocity impact testing, analytic impact predictors, and hydrodynamic codes. Among these tools, perhaps the most accepted is impact testing, which has the advantage of providing actual verification of spacecraft designs. On the other hand, maximum test velocities are currently limited (8 km/s) relative to maximum space debris (about 15 km/s) and meteoroid (about 72 km/s) velocities. Also, a great deal of (often expensive) testing is required to develop statistically significant trends for the large number of parameters associated with hypervelocity

Received Dec. 15, 1989; presented as Paper 90-0087 at the 28th Aerospace Sciences Meeting, Reno, NV, Jan. 8-11, 1990; revision received July 2, 1990; accepted for publication July 3, 1990. Copyright © 1990 by the American Institute of Aeronautics and Astronautics, Inc. All rights reserved.

*Systems Survivability Engineer. Member AIAA.

impact. Hydrodynamic code analysis can overcome the velocity limitation problem. However, this method is very computer (and time) intensive, and there is a fair amount of controversy involved in the selection of appropriate codes and code-specific parameters.

Analytic impact predictors generally provide the best quick-look estimate of design tradeoffs. Their use is constrained by the limitations of the testing from which they are experimentally derived, the assumptions used in their theoretical derivation, or the regression analysis used in their statistical formation. However, analytic predictors may provide information that is clearer than that obtained from the examination of experimental results.

The most complete way to determine the characteristics of an analytic impact predictor is through (nonlinear) optimization of the protective structures design problem formulated with the predictor of interest. Optimization techniques provide analytic or curve optimal profiles depending on the nature of the predictor, the problem formulation, and the technique used.⁸

The objective of this paper is to present a unique design optimization methodology for protective structures of spacecraft subject to meteoroid and space debris environs. This technique is formulated around geometric programming,⁹ but also includes penalty function and search techniques. Optimization is used here to describe the process of determining the structural thicknesses and materials that will minimize protective structures weight for a given mission and risk level. Results will be confined to the Space Station core module configuration (CMC) and the space debris environment, which dominates the meteoroid environment for long-term and large spacecraft missions.

B. Scope and Method of Approach

The protective structures design optimization problem discussed here is confined to the Space Station core module configuration and space debris environment with the following baseline parameters: 5% space debris growth rate; Space Station operation period from 1995–2004; 460-km Space Station altitude; 28.5 deg Space Station inclination; 0.97 total core module configuration probability of no penetration; 588 m² total core module configuration debris area; 10-cm bumper/wall separation; 6061-T6 aluminum alloy bumper; and 2219-T87 aluminum alloy wall. These baseline parameters were selected as representative of the current space debris environment and Space Station configuration/mission for NASA-MSFC Contract NAS8-37378, "Optimization Techniques Applied to Passive Measures for In-Orbit Spacecraft Survivability."¹¹ Parametrics on most of these variables are included to develop design sensitivities for this mission.

Because other studies have focused on analyzing existing protective structures designs, the methodology presented here is a unique one. It results in the risk-adjusted design optimization of protective structures over three hypervelocity impact physics regions: ballistic, projectile shatter, and projectile melt/vaporization. The process begins with the space debris environment definition. The critical design projectile diameter, density, and velocity probability distribution are determined from the space debris growth rate, the spacecraft operational period, mission altitude and inclination, spacecraft area, and probability of no penetration.

The design problem is then formulated for each of the three impact region subpredictors as a weight minimization problem in terms of the independent (or designer controllable) variables. These variables may change depending on the intent of the study, but they generally include bumper/wall material properties and thicknesses.

The three subpredictor designs, corresponding to the three impact physics regions, are then individually optimized for fixed velocities and their corresponding impact angle. An interface algorithm is applied to determine which subpredictor design dominates for a given velocity. Finally, the design is

stochastically integrated over the range of velocities using the velocity probability distribution for the critical design projectile. This produces the overall risk-optimized structural design for the spacecraft.

II. Space Debris Environment Model

A. Introduction

The space debris environment model chosen for this paper is due to Kessler et al.¹⁰ The major dependencies considered involve space debris growth rate, spacecraft operational period, mission altitude and inclination, spacecraft debris area, orientation and probability of no penetration.

B. Flux and Projectile Diameter Solution

The space debris flux is given by Kessler as

$$F(D, h, i, t, s) = B \phi(h, s) \Psi(i) [F_1(D) g_1(t) + F_2(D) g_2(t)] \quad (1)$$

where

$$\phi(h, s) = \phi_1(h, s) / [\phi_1(h, s) + 1] \quad (2)$$

$$\phi_1(h, s) = 10^{(h/200 - s/140 - 1.5)} \quad (3)$$

$$F_1(D) = 1.05(10^{-5})/D^{2.5} \quad (4)$$

$$F_2(D) = 7.0(10^{10})/(D + 700)^6 \quad (5)$$

$$g_1(t) = (1 + 2p)^{t-1985} \quad (6)$$

$$g_2(t) = (1 + p)^{t-1985} \quad (7)$$

The spacecraft inclination factor for 28.5 deg is 0.9135. The cumulative flux N is given by

$$N = \int_0^T FA \, dt \quad (8)$$

which may be approximated using one-year intervals by

$$N = A \sum_{t=t_i}^{t_f} F[D, h, i, t, s(t)] \quad (9)$$

A Poisson arrival rate for space debris gives

$$P_0 = e^{-N} \quad (10)$$

A closed-form solution for D may be accurately found for particle diameters much smaller than 700 cm. This is given by

$$D = \left[\frac{1.05(10^{-5})(G_1)}{-5.9499(10^{-7})G_2 - \frac{\ln(P_0)}{AB\Psi(i)}} \right]^{0.4} \quad (11)$$

where

$$G_j = \sum_{t=t_i}^{t_f} \phi[h, s(t)] g_j(t) \quad \text{for } j = 1, 2 \quad (12)$$

C. Projectile Mass Density

The average projectile mass density is given in gm/cm³ by Kessler as

$$\rho_p = 2.8 \quad \text{for } D \leq 1 \text{ cm} \quad (13)$$

$$\rho_p = 2.8/D^{0.74} \quad \text{for } D > 1 \text{ cm} \quad (14)$$

This relationship is shown in Fig. 1.

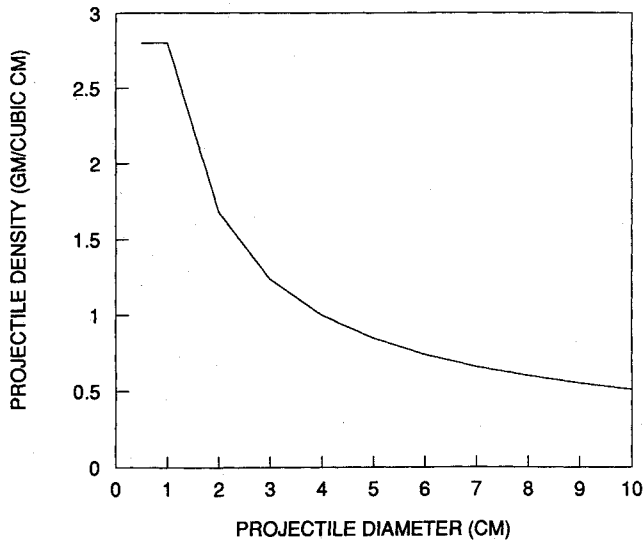


Fig. 1 Space debris particle density vs diameter.

D. Impact Velocity/Angle Distribution

For an orbital inclination of 28.5 deg, the non-normalized impact velocity distribution is given by

$$f(V) = (14.46V - V^2) \{ 18.7e^{-[(V-18.07)/3.614]^2} + 0.67e^{-[(V-9.505)/3.925]^2} \} + 0.0116(28.91V - V^2) \quad (15)$$

The normalized impact velocity distribution is given by

$$f_n(V) = \frac{f(V)}{\int_0^\infty f(V) dV} \quad (16)$$

This distribution is shown in Fig. 2 for $i = 28.5$ deg. Finally, the impact angle is given as a function of impact velocity as

$$\theta = \cos^{-1}(-V/15.4) \quad (17)$$

This relationship is shown (with uncertainty bounds) in Fig. 3 for a surface parallel to the CMC velocity vector.

III. Protective Structures Design Optimization

A. Introduction

The optimization problem is formulated and solved for the ballistic, projectile shatter, and projectile melt/vaporization impact regions in Subsecs. B, C, and D. These optimal solutions are then integrated into an overall optimal solution in Sec. E. The basic optimization problem is a weight minimization problem of the protective structures. It has been shown⁸ that for spacecraft structures with low curvature and relatively large diameter, it is sufficient to minimize the total mass per unit area given by

$$W = \sum_{i=1}^2 \rho_i t_i \quad (18)$$

In particular, this is true for the Space Station core module configuration. Increasing the complexity of the weight objective function by accounting for specific configurations only serves to increase the complexity of the optimization technique and convergence time unnecessarily. No improvement in accuracy is achieved. The predictor equations chosen are based on previous work performed by Boeing.¹² The ballistic, projectile shatter, and projectile melt/vaporization predictors are given by the PEN4,¹² Burch,¹³ and Wilkinson⁶ models, respectively.

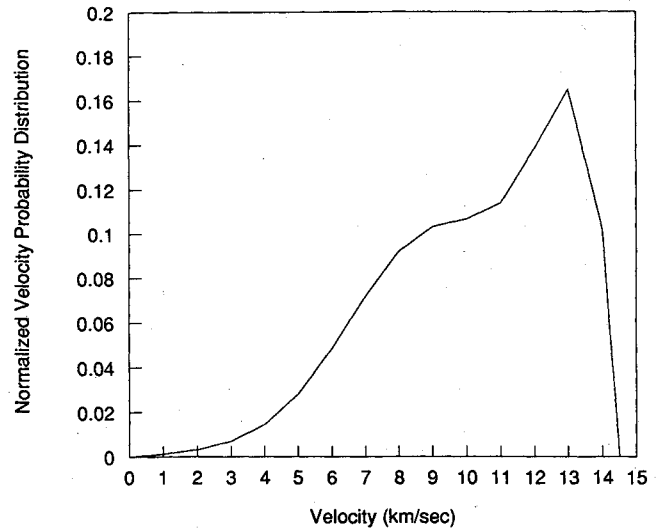


Fig. 2 Velocity probability distribution for 28.5-deg inclination.

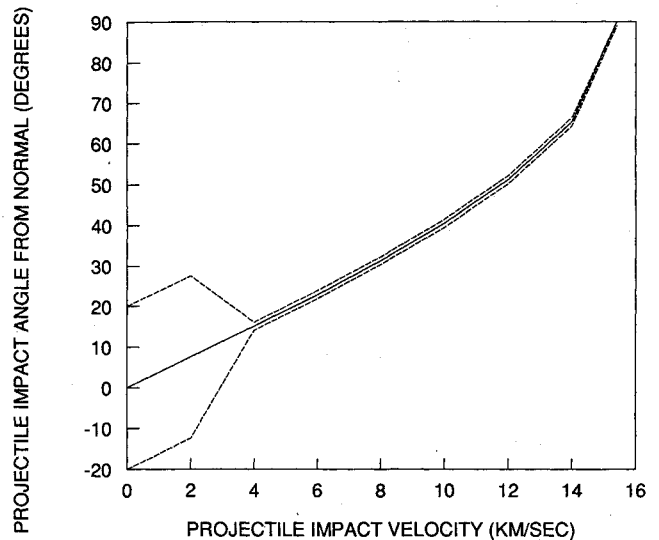


Fig. 3 Projectile impact angle from normal of surface oriented parallel to CMC velocity vector vs impact velocity.

B. Ballistic Impact Predictor

The PEN4¹² model in functional form is given by the following set of equations:

$$t_2 = 1.67 \left(\frac{c_1 \rho_p}{2S_{y_2}} \right)^{0.31} \left(\frac{0.281 D \rho_p}{\rho_2} \right)^{1/3} \cos(\theta) \quad (19)$$

$$c_1 = \frac{a - b}{c + d} \quad (20)$$

$$a = 1.33 V^2 R_p^2 \rho_p^2 \quad (21)$$

$$b = 8S_{y_1} t_1 e^{-3.125(10^{-4})V/\cos(\theta)} \quad (22)$$

$$c = 1.33 R_p^2 \rho_p \quad (23)$$

$$d = R_p t_1 \rho_1 / \cos(\theta) \quad (24)$$

This set of equations is valid for

$$V \leq V_f + 4000 \quad (25)$$

where

$$V_f = 4100 \quad \text{if} \quad t_1/D \leq 0.4 \quad (26)$$

$$V_f = 4986(t_1/D)^{0.21} \quad \text{if} \quad t_1/D > 0.4 \quad (27)$$

When Eqs. (19–24) are substituted into Eq. (18), a one-dimensional search is performed on t_1 with initial point

$$t_1 = 0.16625 V^2 R_p^2 \rho_p \cos(\theta) \frac{e^{3.125(10^{-4})V}}{S_{y_1}} \quad (28)$$

corresponding to $t_2 = 0$. When a local optimal solution is determined, condition (25) is checked to determine if the ballistic region is appropriate for consideration.

C. Projectile Shatter Predictor

The Burch¹³ model is actually two separate predictors: one for normal impacts, and one for oblique impacts. The normal impact predictor is given in functional form as

$$t_2 = \frac{(F_1 D/N)^{1.71} (C/V)^{2.29}}{S^{0.71}} \quad (29)$$

where

$$F_1 = 2.42(t_1/D)^{-0.33} + 4.26(t_1/D)^{0.33} - 4.18 \quad (30)$$

Equation (30) may be approximated by

$$\bar{K} = F_1^{1.71} = 2.8(t_1/D)^{0.57} + 1.58(t_1/D)^{-0.57} \quad (31)$$

Then W is given in posynomial form as

$$W = \rho_1 t_1 + \rho_2 \bar{C} \bar{K} \quad (32)$$

where

$$\bar{C} = \frac{(D/N)^{1.71} (C/V)^{2.29}}{S^{0.71}} \quad (33)$$

The dual geometric programming problem is to maximize

$$v(\delta) = (\rho_1/\delta_1)^{\delta_1} \left(\frac{2.8\rho_2 \bar{C} D^{-0.57}}{\delta_2} \right)^{\delta_2} \left(\frac{1.58\rho_2 \bar{C} D^{0.57}}{\delta_3} \right)^{\delta_3} \quad (34)$$

subject to

$$\delta_1 + 0.57\delta_2 - 0.57\delta_3 = 0 \quad (35)$$

$$\sum_{i=1}^3 \delta_i = 1 \quad (36)$$

Equations (35) and (36) may be partially solved to give

$$\delta_2 = 2.33(1 - 1.57\delta_3) \quad (37)$$

$$\delta_1 = 1.33(2\delta_3 - 1) \quad (38)$$

Since the dual variables must all be positive, we have

$$0.5 < \delta_3 < 0.64 \quad (39)$$

Thus, the one-degree-of-difficulty algorithm is given by:

1) Vary δ_3 from 0.5 to 0.64 to find the max $v(\delta)$.

2) Using the corresponding δ_3 , solve for δ_1 , and δ_2 .

$$3) t_{10} = \frac{\delta_1 v_0(\delta)}{\rho_1}$$

$$4) t_{20} = \frac{v_0(\delta) - \rho_1 t_{10}}{\rho_2}$$

The oblique Burch predictor is formulated in terms of flight-path and normal-path penetration as

$$t_2 = D \left(\frac{F_1 + 0.63F_2}{N_F} \right)^{12/7} \left(\frac{C}{V} \right)^{16/7} \left(\frac{D}{S} \right)^{5/7} \quad (40)$$

where F_1 is as defined in Eq. (30) and

$$F_2 = 0.5 - 1.87(t_1/D) + (5t_1/D - 1.6)\chi^3 + (1.7 - 12t_1/D)\chi \quad (41)$$

$$\chi = \tan(\theta) - 0.5 \quad (42)$$

The weight minimization problem may then be formulated as

$$W = \rho_1 t_1 + \rho_2 t_2 \quad (43)$$

subject to

$$N_N \leq 0.85 \quad (44)$$

where

$$N_N = F_3(D/t_2)(C/V)^{4/3} \quad (45)$$

$$F_3 = 0.32(t_1/D)^{5/6} + 0.48(t_1/D)^{1/3} \sin^3(\theta) \quad (46)$$

and t_2 is given by Eq. (40). This problem is solved using an exterior penalty function technique with objective function

$$\phi(t_1) = W + \delta K(N_N - 0.85)^2 \quad (47)$$

where

$$\delta = 1 \quad \text{if} \quad N_N - 0.85 \geq 0 \quad (48)$$

$$\delta = 0 \quad \text{if} \quad N_N - 0.85 < 0 \quad (49)$$

A random search with a 99% confidence interval of 0.01 in. is performed, and K is increased until

$$\delta K(N_N - 0.85)^2 \leq \epsilon \quad (50)$$

The random search interval for t_1 is specified by using the single plate equation

$$t_1 = K_1 m^{0.352} \rho_p^{1/6} V^{0.875} \quad (51)$$

Table 1 Comparison of aluminum alloy bumper materials

Aluminum alloy	t_{10} , cm	t_{20} , cm	W_0 , kg
2219-T87	0.46	0.65	5715
1100-H18	0.50	0.64	5839
2011-T8	0.46	0.64	5665
2014-T6	0.44	0.71	5910
2024-T81	0.44	0.72	5929
5005-H18	0.49	0.64	5760
5050-H38	0.49	0.64	5768
5052-H38	0.49	0.65	5748
5056-H38	0.49	0.66	5762
5083-O	0.53	0.65	5978
5086-O	0.55	0.65	6059
5154-H38	0.49	0.65	5769
5357-H38	0.48	0.64	5737
5456-O	0.52	0.65	5942
6061-T6	0.48	0.64	5695
6063-T6	0.48	0.64	5737
6101-T6	0.49	0.64	5760
6151-T6	0.48	0.65	5719
7075-T6	0.43	0.71	5858

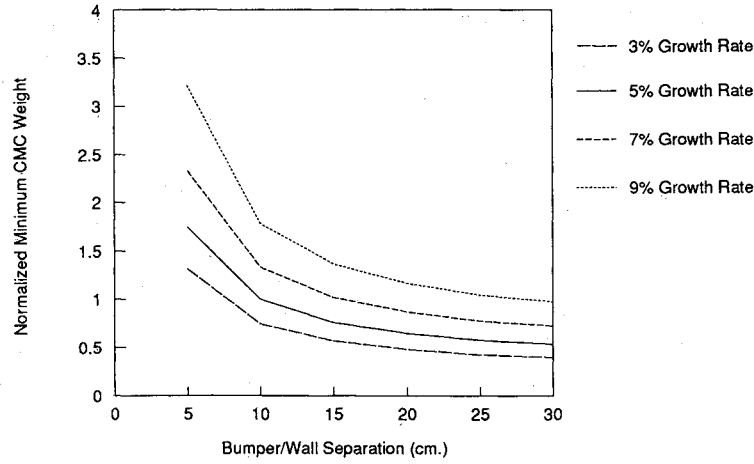


Fig. 4 Minimum core module weight vs bumper wall separation for various space debris growth rates (2011-T8 aluminum).

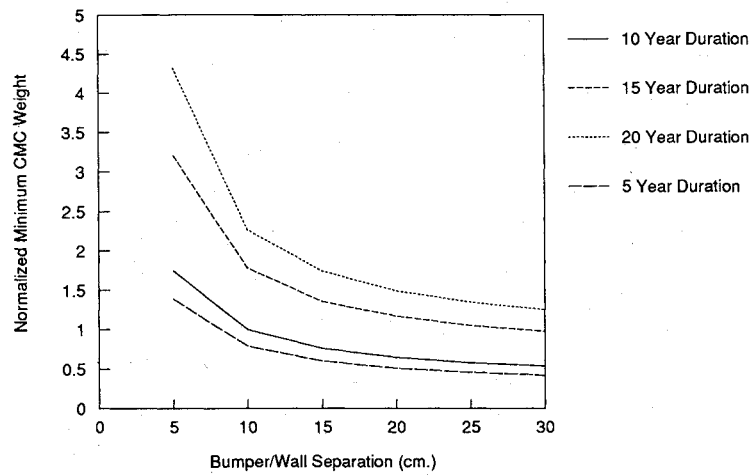


Fig. 5 Minimum core module weight vs bumper wall separation for various CMC durations (2011-T8 aluminum).

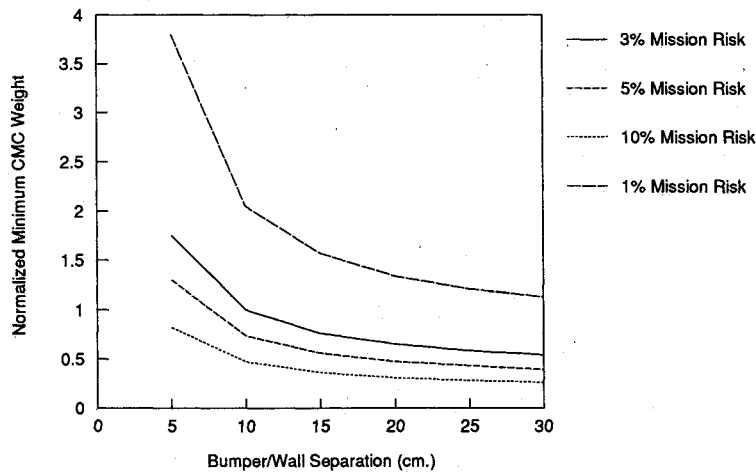


Fig. 6 Minimum core module weight vs bumper wall separation for various CMC mission risks (2011-T8 aluminum).

$$K_1 = \frac{0.816}{e^{1/18} \rho_1^{1/2}} \quad (52)$$

The interval is then given by $[0, t_1]$.

D. Projectile Melt/Vaporization Predictor

The Wilkinson⁶ predictor is given by

$$t_2 = \frac{0.364 D^3 \rho_p V \cos(\theta)}{L_2 S^2 \rho_2} \quad \text{for} \quad \frac{D \rho_p}{\rho_1 t_1} \leq 1 \quad (53)$$

$$t_2 = \frac{0.364 D^4 \rho_p^2 V \cos(\theta)}{L_2 S^2 \rho_1 t_1 \rho_2} \quad \text{for} \quad \frac{D \rho_p}{\rho_1 t_1} > 1 \quad (54)$$

Under condition (54), the dual geometric programming objective function is given by

$$\nu(\delta) = (\rho_1 / \delta_1)^{\delta_1} (c_1 / \delta_2)^{\delta_2} \quad (55)$$

$$c_1 = \frac{0.364 D^4 \rho_p^2 V \cos(\theta)}{L_2 S^2 \rho_1} \quad (56)$$

$$\delta_1 + \delta_2 = 1 \quad (57)$$

$$\delta_1 - \delta_2 = 0 \quad (58)$$

Equations (57) and (58) together imply

$$\delta_1 = \delta_2 = 1/2 \quad (59)$$

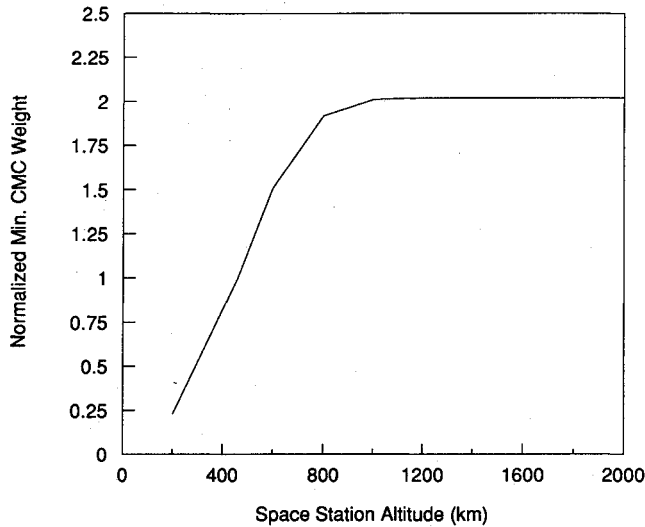


Fig. 7 Minimum core module weight vs space station altitude (2011-T8 aluminum).

The minimum weight and globally optimal thicknesses are given by

$$W_0 = \frac{1.207 D^2 \rho_p \left[\frac{V \cos(\theta)}{L_2} \right]^{1/2}}{S} \quad (60)$$

$$t_{10} = \frac{0.604 D^2 \rho_p \left[\frac{V \cos(\theta)}{L_2} \right]^{1/2}}{S \rho_1} \quad (61)$$

$$t_{20} = \frac{0.604 D^2 \rho_p \left[\frac{V \cos(\theta)}{L_2} \right]^{1/2}}{S \rho_2} \quad (62)$$

Thus, the globally optimal algorithm for the Wilkinson predictor is

- 1) Determine t_{10} and t_{20} from Eqs. (61) and (62).
- 2) Compute $(D\rho_p)/(\rho_1 t_{10})$.
- 3) If $(D\rho_p)/(\rho_1 t_{10}) > 1$, then quit. The optimal design is (t_{10}, t_{20}) .
- 4) If $(D\rho_p)/(\rho_1 t_{10}) \leq 1$, the optimal design is

$$\left[t_{10}, t_{20} \left/ \left(\frac{D\rho_p}{\rho_1 t_{10}} \right) \right. \right]$$

E. Integrating the Three Impact Regions

Due to the discontinuities existing between the three impact predictors, an integrating algorithm must be developed. This algorithm is included for fixed velocities.

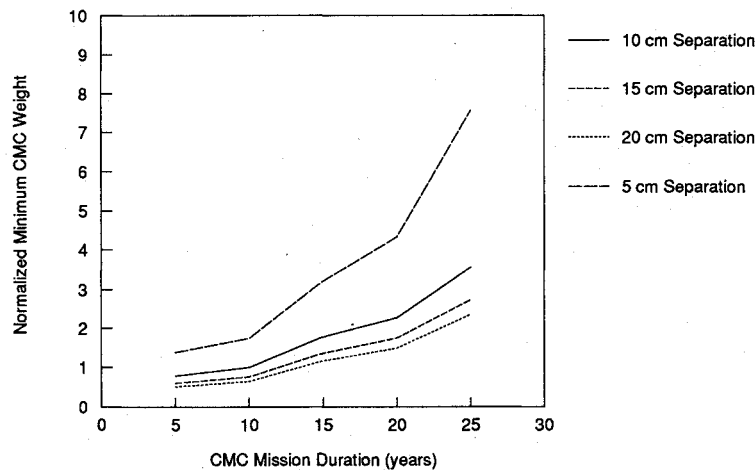


Fig. 8 Minimum core module weight vs CMC mission duration for various CMC bumper wall separations (2011-T8 aluminum).

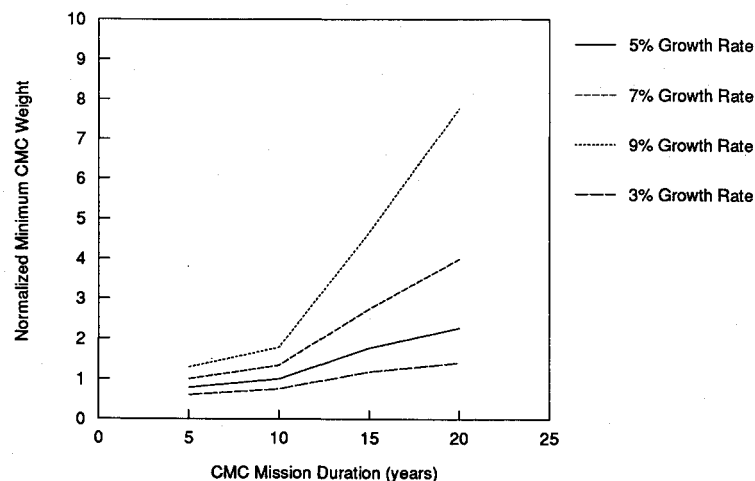


Fig. 9 Minimum core module weight vs CMC mission duration for various space debris growth rates (2011-T8 aluminum).

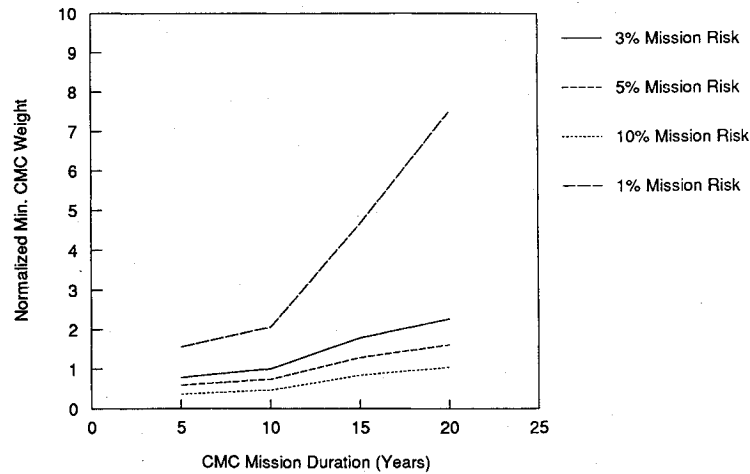


Fig. 10 Minimum core module weight vs CMC mission duration for various CMC mission risks (2011-T8 aluminum).

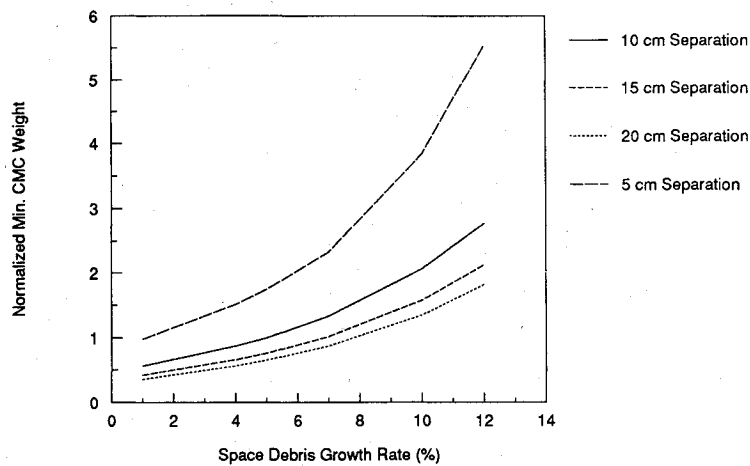


Fig. 11 Minimum core module weight vs space debris growth rate for various bumper/wall separations (2011-T8 aluminum).

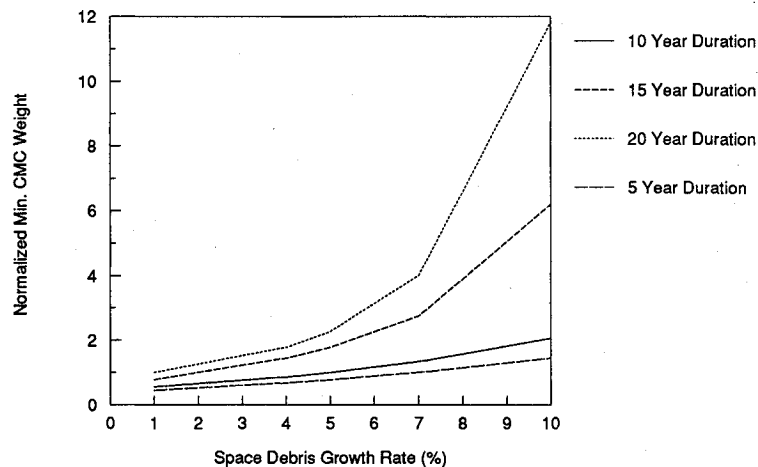


Fig. 12 Minimum core module weight vs space debris growth rate for various CMC mission durations (2011-T8 aluminum).

- 1) Compute optimal design for PEN4 predictor (t_{10p}, t_{20p}) .
- 2) Check against PEN4 constraint Eq. (25).
- 3) If satisfied, the optimal design is $(t_{10}, t_{20}) = (t_{10p}, t_{20p})$.
- 4) Otherwise, compute optimal designs for Burch and Wilkinson predictors (t_{10B}, t_{20B}) and (t_{10W}, t_{20W}) , respectively.
- 5) Compute Wilkinson wall induced by optimal Burch bumper $t_{2W}(t_{10B})$.
- 6) Compute Burch wall induced by optimal Wilkinson bumper $t_{2B}(t_{10W})$.

7) Find $(t_{10}, t_{20}) = \min_{\rho_1 t_1 + \rho_2 t_2} (\{t_{10B}, \max[t_{20B}, t_{2W}(t_{10B})]\}, \{t_{10W}, \max[t_{20W}, t_{2B}(t_{10W})]\})$.
Once the optimal bumper and wall thicknesses are determined for each velocity, the integrated optimal bumper and wall thicknesses are found from

$$t_{i0} = \int_0^{V_{\max}} t_{i0}[V, \theta(V)] f_n(V) dV \quad \text{for } i = 1, 2 \quad (63)$$

IV. Protective Structures Design Tradeoffs

A. Bumper Material

The sensitivity of optimal protective structures design to variations in the aluminum alloy bumper material is shown in Table 1 for the baseline parameters given in Sec. I.B. Note the wide variation in core module weight. The optimal aluminum alloy for the baseline parameters is 2011-T8.

B. Bumper/Wall Separation

Several design parametrics for bumper/wall separation are shown in Figs. 4–6 for 2011-T8 aluminum. The tradeoffs are

normalized to the optimal design for 2011-T8 given in Table 1. These parametrics show that there is a weight incentive of roughly 25% for increasing this separation to 15 cm. However, further increases in bumper/wall separation produce decreasing weight savings. Alternatively, decreasing the bumper/wall separation to 5 cm results in a 75% weight increase.

C. Space Station Altitude

The sensitivity of CMC protective structures design to Space Station altitude is shown in Fig. 7 for 2011-T8 aluminum. This parametric shows a large design sensitivity to altitude in the

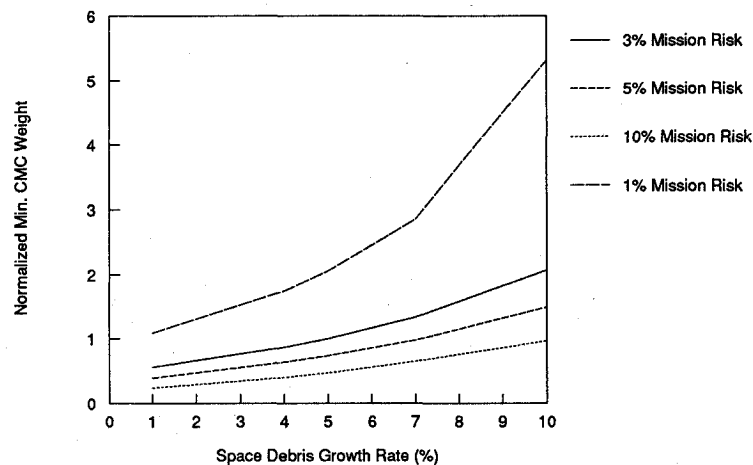


Fig. 13 Minimum core module weight vs space debris growth rate for various CMC mission risks (2011-T8 aluminum).

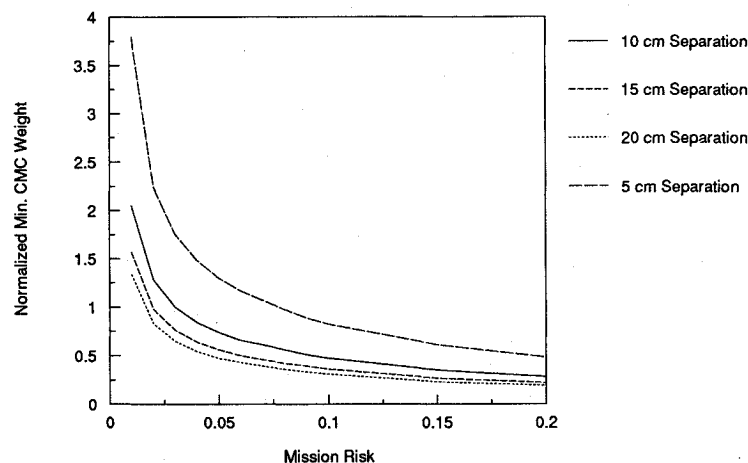


Fig. 14 Minimum core module weight vs CMC mission risk for various bumper/wall separations (2011-T8 aluminum).

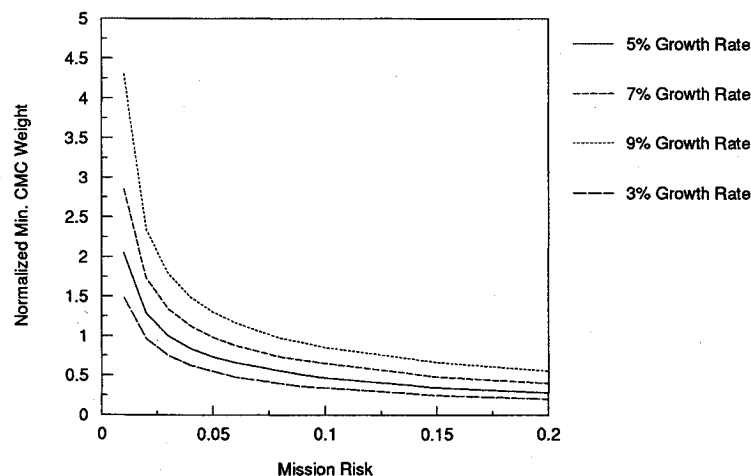


Fig. 15 Minimum core module weight vs CMC mission risk for various space debris growth rates (2011-T8 aluminum).

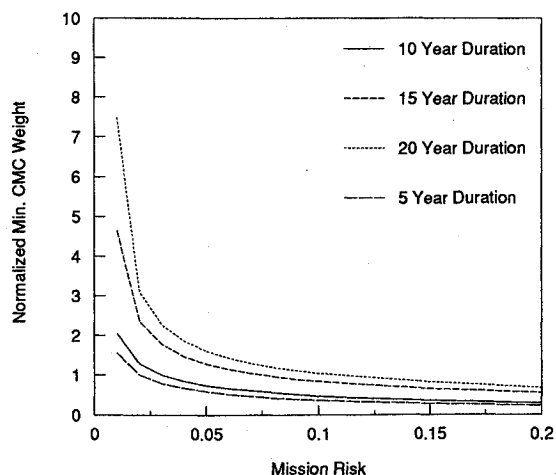


Fig. 16 Minimum core module weight vs CMC mission risk for various CMC mission durations (2011-T8 aluminum).

300 to 600 km range. Furthermore, Space Station altitude effects are relatively small above 1000 km where the design weight is twice that for the baseline parameters.

D. CMC Mission Duration

Several design parametrics for CMC mission duration are shown in Figs. 8–10 for 2011-T8 aluminum. These parametrics show that there is a large weight sensitivity (25%) to mission duration above approximately 10 yr. In particular, a 15-yr duration is particularly stressing due to unfavorable solar flux effects.

E. Space Debris Growth Rate

Several design parametrics for space debris rate are shown in Figs. 11–13 for 2011-T8 aluminum. These parametrics show that there is a high weight sensitivity to space debris growth rate above approximately 7%. In fact, a 3% increase in the space debris growth rate (from 5 to 8%) results in a 50% increase in minimum weight.

F. CMC Mission Risk

Several design parametrics for CMC mission risk are shown in Figs. 14–16 for 2011-T8 aluminum. Mission risk is defined as 1 minus the probability of no penetration. These parametrics show that there is a weight incentive of roughly 25% for increasing mission risk from 3 to 5%. Furthermore, there is a weight penalty of about 30% for decreasing mission risk to 2%.

V. Conclusions and Recommendations

A. Conclusions

The use of nonlinear optimization techniques combined with analytic impact predictors provides quick designer trade-off studies that may be used in conjunction with hypervelocity impact testing, hydrodynamic analysis, and other engineering design functions. In particular, global nonlinear optimization can be performed for the projectile melt/vaporization region and for normal impacts in the projectile shatter region using geometric programming. For those model situations in which geometric programming is not applicable, other nonlinear optimization techniques, including penalty function and search techniques, can be used satisfactorily.

A number of results specific to the Space Station core module configuration and mission have been reached using

this methodology. In particular, 2011-T8 is the preferable aluminum alloy bumper choice (of those investigated) for the baseline parameters. Additionally, increasing the bumper/wall separation from 10 to 15 cm reduces the minimum module weight by 50%. The minimum CMC weight is very sensitive to space debris growth rate above 7% and Space Station altitude below 1000 km. Furthermore, the CMC protective structures design depends greatly on mission duration. Finally, increasing the CMC mission risk from 3 to 5% reduces the minimum module weight by about 30%.

B. Recommendations

A number of additional analyses could be carried out using this methodology. In particular, alternate metallic bumper materials should be investigated using this method, impact testing, hydrodynamic analysis, and other available techniques. Additionally, uncertainty analyses should be performed relative to the space debris environment parameters. Posynomial regression analysis should be performed for the projectile shatter region to take advantage of the geometric programming optimization technique. Furthermore, a combined meteoroid/space debris optimization algorithm should be implemented. Finally, advanced materials (e.g., composites, "smart materials") should be investigated.

Acknowledgments

I would like to thank Sherman Avans and Jennifer Horn of the Marshall Space Flight Center for their direction and contributions to this development under NASA Contract NAS8-37378. I also wish to thank Mary Price of SAIC for introducing me to the geometric programming technique.

References

- ¹Cour-Palais, B., "Meteoroid Environment Model—1969 (Near-Earth to Lunar Surface)," NASA SP-8013, March 1969.
- ²Susko, M., "A Review of Micrometeoroid Flux Measurements and Models for Low Orbital Altitudes of the Space Station," NASA TM-86466, Sept. 1984.
- ³Madden, R., "Ballistic Limit of Double-Walled Meteoroid Bumper Systems," NASA TN-3916, April 1967.
- ⁴Nysmith, C. R., "An Experimental Impact Investigation of Aluminum Double-Sheet Structures," *Proceedings of the AIAA Hypervelocity Impact Conference*, AIAA Paper 69-375, AIAA, New York, May 1990.
- ⁵Swift, H. F., "Designing Dual-Plate Meteoroid Shields—A New Analysis," Jet Propulsion Laboratory, Pasadena, CA, Publ. 82-39, March 1982.
- ⁶Wilkinson, J. P. D., "A Penetration Criterion for Double-Walled Structures Subject to Meteoroid Impact," *AIAA Journal*, Vol. 7, No. 10, 1969, pp. 1937–1943.
- ⁷Richardson, A. J., "Development of Dual Bumper Wall Construction for Advanced Spacecraft," *Journal of Spacecraft and Rockets*, Vol. 9, No. 6, 1972, pp. 448–451.
- ⁸Mog, R. A., Lovett, J. N., and Avans, S. L., "Global Nonlinear Optimization of Spacecraft Protective Structures Design," NASA TM-100387, Jan. 1990.
- ⁹Gottfried, B. S., and Weisman, J., *Introduction to Optimization Theory*, Prentice-Hall, Englewood Cliffs, NJ, 1973, pp. 265–282.
- ¹⁰Kessler, D., Reynolds, R., and Anz-Meador, P., "Orbital Debris Environment for Spacecraft Designed to Operate in Low Earth Orbit," NASA TM-100471, April 1989.
- ¹¹Mog, R. A., and Price, D. M., "Optimization Techniques Applied to Passive Measures for In-Orbit Spacecraft Survivability—Final Report," Contract NAS8-37378, Nov. 1987.
- ¹²Coronado, A. R., Gibbins, M. N., Wright, M. A., and Stern, P. H., "Space Station Integrated Wall Design and Penetration Damage Control," Boeing Aerospace Co. Final Rept., Contract NAS8-36426, July 1987.
- ¹³Burch, G. T., Air Force Armament Lab. Tech. Rept. AFATL-TR-67-116, Boeing, 1967.

David H. Allen
Associate Editor